

# Genetic profiles of subcutaneous panniculitis-like T-cell lymphoma and clinicopathological impact of *HAVCR2* mutations

Jiwon Koh,<sup>1</sup> Insoon Jang,<sup>2</sup> Seungchan Mun,<sup>3-5</sup> Cheol Lee,<sup>1</sup> Hee Jeong Cha,<sup>6</sup> Young Ha Oh,<sup>7</sup> Jin-Man Kim,<sup>8</sup> Jae Ho Han,<sup>9</sup> Jin Ho Paik,<sup>10</sup> Junhun Cho,<sup>11</sup> Young Hyeon Ko,<sup>11</sup> Chan-Sik Park,<sup>12</sup> Heounjeong Go,<sup>12</sup> Jooryung Huh,<sup>12</sup> Kwangsoo Kim,<sup>2,13</sup> and Yoon Kyung Jeon<sup>1,3,5</sup>

<sup>1</sup>Department of Pathology, Seoul National University Hospital, Seoul National University College of Medicine, Seoul, Republic of Korea; <sup>2</sup>Department of Data Science Research, Innovative Medical Technology Research Institute, Seoul National University Hospital, Seoul, Republic of Korea; <sup>3</sup>Seoul National University Cancer Research Institute, Seoul, Republic of Korea; <sup>4</sup>Interdisciplinary Graduate Program in Cancer Biology, Seoul National University College of Medicine, Seoul, Republic of Korea; <sup>5</sup>Integrated Major in Innovative Medical Science, Seoul National University Graduate School, Seoul, Republic of Korea; <sup>6</sup>Department of Pathology, Ulsan University Hospital, Ulsan University College of Medicine, Ulsan, Republic of Korea; <sup>7</sup>Department of Pathology, Hanyang University Guri Hospital, Hanyang University College of Medicine, Guri, Gyeonggi-do, Republic of Korea; <sup>8</sup>Department of Pathology, College of Medicine, Chungnam National University, Daejeon, Republic of Korea; <sup>9</sup>Department of Pathology, Ajou University School of Medicine, Suwon, Gyeonggi-do, Republic of Korea; <sup>10</sup>Department of Pathology, Seoul National University Bundang Hospital, Seoul National University College of Medicine, Seongnam, Gyeonggi-do, Republic of Korea; <sup>11</sup>Department of Pathology, Samsung Medical Center, Sungkyunkwan University School of Medicine, Seoul, Republic of Korea; <sup>12</sup>Department of Pathology, Asan Medical Center, University of Ulsan College of Medicine, Seoul, Republic of Korea; and <sup>13</sup>Transdisciplinary Department of Medicine & Advanced Technology, Seoul National University Hospital, Seoul, Republic of Korea

## Key Points

- *HAVCR2*<sup>Y82C</sup> mutation was found in 51% of SPTCL cases and was associated with younger age, systemic illness, and shorter RFS.
- *HAVCR2*<sup>Y82C</sup> SPTCLs were enriched in inflammatory signaling, and *HAVCR2*<sup>WT</sup> SPTCLs showed higher *CCR4* expression in the microenvironment.

Recent studies identified germline mutations in *HAVCR2* (encoding T-cell immunoglobulin mucin 3) as a genetic factor that predisposes to subcutaneous panniculitis-like T-cell lymphoma (SPTCL). However, the differences between *HAVCR2*-mutated (*HAVCR2*<sup>MUT</sup>) and *HAVCR2* wild-type (*HAVCR2*<sup>WT</sup>) SPTCLs remain unclear. A nationwide cohort of 53 patients with SPTCL diagnosed at 8 Korean institutions was established. Whole-exome sequencing and RNA-sequencing were performed on 8 patients in the discovery set. In the validation set, targeted gene sequencing or direct sequencing of *HAVCR2* was performed. Of 49 patients with available *HAVCR2* status, 25 (51.0%) were *HAVCR2*<sup>Y82C</sup>. *HAVCR2*<sup>Y82C</sup> was associated with younger age ( $P = .001$ ), development of hemophagocytic lymphohistiocytosis or hemophagocytic lymphohistiocytosis-like systemic illness ( $P < .001$ ), and short relapse-free survival (RFS) ( $P = .023$ ). Most mutated genes in SPTCLs were involved in immune responses, epigenetic modifications, and cell signaling. Mutations in *UNC13D*, *PIAS3*, and *KMT2D* were more frequent in *HAVCR2*<sup>WT</sup> SPTCLs. At the gene expression level, *HAVCR2*<sup>Y82C</sup> SPTCLs were enriched in genes involved in IL6-JAK-STAT3 signaling and in tumor necrosis factor- $\alpha$  signaling via NF- $\kappa$ B. *CCR4* was significantly upregulated in *HAVCR2*<sup>WT</sup> SPTCLs both at the messenger RNA level and at the protein level. We established a risk stratification system for SPTCL by integrating clinical and histopathological features, including age and *HAVCR2* mutation status. This risk stratification system was strongly associated with RFS ( $P = .031$ ). In conclusion, the *HAVCR2*<sup>Y82C</sup> mutation was common in Korean patients with SPTCL and was associated with unique clinicopathological and genetic features. Combining clinicopathological parameters could aid in predicting prognosis for patients with SPTCL.

## Introduction

Subcutaneous panniculitis-like T-cell lymphoma (SPTCL) is a rare T-cell non-Hodgkin lymphoma (NHL) with a cytotoxic phenotype. SPTCLs account for <1% of all NHLs worldwide<sup>1</sup> and 0.3% of all malignant

Submitted 21 February 2021; accepted 10 July 2021; prepublished online on *Blood Advances* First Edition 17 September 2021; final version published online 14 October 2021. DOI 10.1182/bloodadvances.2021004562.

The whole-exome sequencing and RNA-sequencing data sets are available under accession number PRJNA687553 at BioProject.

The full-text version of this article contains a data supplement.

© 2021 by The American Society of Hematology. Licensed under Creative Commons Attribution-NonCommercial-NoDerivatives 4.0 International (CC BY-NC-ND 4.0), permitting only noncommercial, nonderivative use with attribution. All other rights reserved.

lymphomas in the Republic of Korea.<sup>2</sup> SPTCL typically affects young individuals, with a median patient age of 36 years and a female sex bias.<sup>3</sup> Histopathologically, SPTCL is characterized by CD8-positive T cells infiltrating into subcutaneous adipose tissue, with rimmed individual fat cells in a lace-like pattern. Differential diagnoses include lupus panniculitis (LP) and other T-cell NHLs with cutaneous involvement, such as primary cutaneous  $\gamma\delta$  T-cell lymphoma (PCGDTCL) and mycosis fungoides (MF).<sup>4</sup> Patients with SPTCL have an excellent prognosis, with a 5-year overall survival (OS) rate of >80%; however, ~20% of patients with SPTCL develop hemophagocytic lymphohistiocytosis (HLH), which can significantly affect patient survival (5-year OS of 46%).<sup>3</sup>

Recent genetic studies revealed that recurrent germline mutations in *HAVCR2* were present in 25% to 85% of patients with SPTCLs.<sup>5-7</sup> *HAVCR2* encodes T-cell immunoglobulin mucin 3 (TIM-3) protein, a critical checkpoint molecule that regulates inflammatory responses.<sup>8</sup> Y82C, I97M, and T101I are common recurrent germline *HAVCR2* mutations in SPTCLs, impairing TIM-3 protein folding, cellular expression, and function.<sup>5</sup> Defective TIM-3 leads to persistent inflammatory responses and potentially causes HLH. Compared with wild-type *HAVCR2* (*HAVCR2*<sup>WT</sup>) SPTCLs, *HAVCR2*-mutated (*HAVCR2*<sup>MUT</sup>) SPTCLs are more frequent in younger individuals and are often associated with HLH; nevertheless, these findings could not be confirmed in a cohort of 13 Asian subjects with SPTCLs.<sup>6</sup>

Although identification of germline mutations that cause SPTCLs provided a deeper insight into the mechanisms underlying SPTCLs, their pathogenesis has not been fully elucidated. Except for *HAVCR2* mutations, no recurrent genetic alterations have been associated with SPTCLs, and the biological mechanisms underlying *HAVCR2*<sup>WT</sup> SPTCLs remain largely unknown. In addition, it is unclear whether *HAVCR2* alterations are specific to SPTCLs or if they are also found in other diseases with panniculitic presentation.

To address these unresolved questions, we established a nationwide multicenter cohort composed of Korean patients with SPTCLs and performed the first genetic study on this population. After a comprehensive review of the clinical and histopathological features, we investigated the mutational spectrum of SPTCLs using whole-exome sequencing (WES), targeted DNA sequencing, and direct sequencing. We compared the mutational patterns of SPTCLs according to *HAVCR2* status and performed RNA-sequencing–based gene expression analysis to identify dysregulated pathways and biological differences between *HAVCR2*<sup>MUT</sup> and *HAVCR2*<sup>WT</sup> SPTCLs, followed by validation on the clinical tissue samples.

## Methods

### Patients and samples

A nationwide multicenter cohort consisting of 53 patients with SPTCL was established (supplemental Table 1); the patients diagnosed at 8 Korean institutions between 1995 and 2020 were screened, and those with available tissue samples for the study were included. Seven patients with LP, 4 patients with PCGDTCL, and 8 patients with MF diagnosed at Seoul National University Hospital (SNUH) were also included; among them, all patients with LP and 3 patients with PCGDTCL exhibited panniculitis-like presentation. All cases were reviewed and diagnosed by experienced hematopathologists in each institute using the revised fourth World Health Organization classification guidelines.<sup>1</sup> Available hematoxylin and eosin slides,

immunohistochemistry (IHC) slides (CD3, CD20, CD4, CD8, CD56, granzyme B, TIA-1, Ki-67, T-cell receptor  $\beta$ F1 [TCR $\beta$ F1], and TCR $\gamma$ ), and Epstein-Barr virus in situ hybridization samples were reviewed by an experienced hematopathologist at SNUH. Clinical information, including bone marrow involvement, HLH or HLH-like systemic illness, relapse-free survival (RFS), OS, and treatment regimens, were collected from the medical records of each institution. HLH was defined according to the HLH-2004 criteria.<sup>9</sup> However, not all institutes were able to run every laboratory test listed in HLH-2004, and thus we designated “HLH-like systemic illness” for those with incomplete criteria for HLH-2004 but clinically regarded as HLH warranting intensive treatment (supplemental Table 2).

This study was approved by the Institutional Review Board of SNUH (approval no. 1809-143-977).

### WES and targeted sequencing

WES was performed by using 9 formalin-fixed, paraffin-embedded samples from 8 patients with SPTCLs, including 1 patient with disease recurrence (patient SP03); all these patients were diagnosed at SNUH (discovery set). Matched non-neoplastic tissue samples were available from 2 patients (SP01 and SP04). Sequencing metrics are summarized in supplemental Table 3.

To evaluate the mutational landscape of SPTCLs, MFs, PCGDTCLs, and LPs, we created a customized panel comprising 208 genes (supplemental Table 4) based on the following criteria: genes with mutations found in >2 patients in the discovery set of this study or previously reported studies on SPTCL<sup>5,6,10,11</sup> (eg, *HAVCR2*, *PIAS3*, *PLCG2*); genes with mutations found in at least 1 patient in the discovery set and known to have functional implications in inflammatory responses or T-cell biology (eg, *IFNL2*, *F5*, *GDF1*); genes with mutations previously reported in CTCLs<sup>12</sup>; and other genes that affect the pathogenesis of lymphoid neoplasms (eg, *RHOA*, *TET2*, *MYD88*). Targeted gene sequencing (TGS) was performed for a total of 32 patients: 20 patients with SPTCL, 8 with MF, 3 with PCGDTCL, and 1 with LP. Details are provided in the supplemental Methods and supplemental Table 5.

### RNA-sequencing and gene expression analysis

RNA-sequencing was performed on 8 samples in the discovery set (supplemental Table 6); 4 were *HAVCR2*<sup>Y82C</sup>, and 4 were *HAVCR2*<sup>WT</sup>. Details are provided in the supplemental Methods.

Genes with median transcripts per million values of <5 were excluded from further analysis. Gene set enrichment analysis (GSEA)<sup>13</sup> between the *HAVCR2*<sup>Y82C</sup> and *HAVCR2*<sup>WT</sup> groups was performed by gene set permutation due to the small sample size.<sup>14</sup> Gene sets from MSigDB (<http://software.broadinstitute.org/gsea/msigdb>)<sup>15</sup> and the SignatureDB collection (<https://lymphochip.nih.gov/signaturedb/>)<sup>16</sup> were used. A cutoff false discovery rate (FDR) q-value  $\leq 0.25$  was used to define significant enrichment.

Next, we defined differentially expressed genes (DEGs) between the *HAVCR2*<sup>Y82C</sup> and *HAVCR2*<sup>WT</sup> groups. DESeq2 analysis<sup>17</sup> was performed on the raw read count matrix after discarding genes with median read counts <5. Genes with an adjusted q-value <0.05 and a  $\log_2$ FC > 2.0 or < -2.0 were regarded as statistically significant.

## Direct sequencing

For those patients who were not suitable for high-throughput sequencing, direct sequencing of *HAVCR2* exon 2 was performed, covering all of the previously reported variants in patients with SPTCL (Y82C, I97M, T101I).<sup>5-7</sup> Details are provided in the supplemental Methods and supplemental Table 7.

## IHC and T-cell clonality test

IHC results were retrieved from the pathology report of each participating institution. During a central review process conducted by SNUH, immunostainings for TCR $\beta$ F1, TCR $\gamma$ , and T-cell clonality test were performed if necessary. To validate the findings from the gene expression analysis, IHC was performed for CCR4, Foxp3, and pSTAT3 on the 4- $\mu$ m-thick whole sections of formalin-fixed, paraffin-embedded tissue samples. CCR4, Foxp3, and pSTAT3 immunostains were digitally scanned and quantified. The positivity for each marker was defined as the percentage of positive cells in the analyzed area. For the 7 selected cases, double-stainings for Foxp3/CCR4 and GATA3/CCR4 were performed. All detailed procedures and manufacturer information are provided in the supplemental Methods.

## Statistical analysis

We used  $\chi^2$ , linear-by-linear, and Fisher's exact tests to compare categorical variables and the Mann-Whitney *U* test to compare continuous variables, as appropriate. Survival analyses were performed by using the log-rank method, and statistical significance was defined as  $P < .05$ . All analyses were performed by using SPSS software (version 25; IBM SPSS Statistics, IBM Corporation, Armonk, NY) and R statistical package 3.6.0 (<http://www.r-project.org>; R Foundation for Statistical Computing, Vienna, Austria).

## Results

### Clinicopathological characteristics

The clinicopathological characteristics of 53 patients with SPTCLs are summarized in Table 1 and supplemental Table 1. The median age at diagnosis was 32 years (range, 8-74 years), and 37 (69.8%) patients were women. Fourteen (28.6%) of 49 patients developed HLH/HLH-like systemic illness, and 15 patients (30.6%) experienced disease relapse. Six (11.8%) of 51 patients died due to disease progression or disease-related complications. Treatment information was available for 43 patients: 33 patients (76.7%) received chemotherapy as first-line treatment, and 10 patients (23.3%) were treated with immunosuppressants. Patients with HLH/HLH-like systemic illness were more likely to be treated with immunosuppressants as first-line therapy ( $P = .017$ ), and there was no differences in the therapeutic approach according to patient age.

We assessed the mutational status of *HAVCR2* using WES, TGS, or direct sequencing (supplemental Tables 1, 8, and 9; Figure 1; supplemental Figure 1). Of 49 patients, 25 had *HAVCR2* Y82C mutation (51.0%), of whom 4 patients harbored heterozygous Y82C mutations. Three of them underwent TGS, and heterozygous status was inferred from the presence of WT alleles and the variant allele frequency (VAF) approximating 50.0% (supplemental Table 9); the other patient (SP14) was tested with direct sequencing, in which WT peak on the electropherogram suggested the heterozygous nature of the mutation. The remainder had homozygous Y82C mutations. *HAVCR2*<sup>Y82C</sup> SPTCLs were more frequent in patients aged <30

years ( $P = .001$ ), and 13 of 14 patients who experienced HLH/HLH-like systemic illness harbored *HAVCR2*<sup>Y82C</sup> ( $P < .001$ ) (Table 1). In contrast to patients with homozygous *HAVCR2*<sup>Y82C</sup>, none of those with heterozygous *HAVCR2*<sup>Y82C</sup> experienced systemic complications (Fisher's exact test,  $P = .031$ ).

Histopathologically, all cases exhibited adipocytic rimming by CD8-positive T cells, regardless of *HAVCR2* status (Figure 1). Tissue necrosis was defined as distinct necrosis with karyorrhectic debris found in at least one high-power field; the necrosis was observed in 41.7% (20 of 48) of patients. Granuloma was noted in 8.3% (4 of 48), and lipogranulomatous inflammation in 16.7% (8 of 48) of patients. Granuloma was more likely to be observed in patients with *HAVCR2*<sup>WT</sup> SPTCLs ( $P = .037$ ).

### Mutational profiles in Korean patients with SPTCLs

WES of nine SPTCL samples revealed a total of 399 nonsynonymous mutations in 342 genes (supplemental Table 8); the median number of variants per case was 55 (range, 2-63). No additional recurrent hotspot mutations other than *HAVCR2*<sup>Y82C</sup> were detected by using WES (supplemental Figure 2). Altered genes were functionally grouped into different categories: T/natural killer (NK) cell-associated inflammation (*HAVCR2*, *PVRL1*, *PVRL4*, *TICAM1*, and *CD4*), epigenetic modifiers (*BAZ2A*, *KMT2D*, and *SETD1A*), and JAK-STAT signaling pathway (*IFNL2* and *PIAS3*). Of note, patient SP04 in the discovery set harbored two point mutations (V272M and K273R) in the same *DDX11* allele, which were confirmed somatic (supplemental Figure 3). Subsequent analyses of samples from patient SP03 revealed 56 mutations in the pretreatment sample (SP03-1) and 50 mutations in the recurrence sample (SP03-2), and 36 mutations were identically shared; remaining variants were found in low VAFs from either one of the samples, suggesting that no significant sequential acquisition or dropout of variants occurred during the clinical course (supplemental Figure 2).

To compare mutation profiles between patients with SPTCLs and other diseases resembling panniculitis, we conducted customized TGS. In total, 588 mutations (median, 8; range, 2-193) in 162 genes were detected in patients with SPTCL (supplemental Table 9). None of the tested samples from patients with MF, PCGDTCL, or LP harbored *HAVCR2* mutations.

Combined WES and TGS analyses indicated that mutations in genes related to immune responses (*ASXL1*, *JAK3*, *PIAS3*, and *PLCG2*) and epigenetic modifiers (*KMT2D*, *KMT2C*, *BAZ2A*, and *NUP98*) were prominent features of SPTCLs (Figure 2). TGS identified *DDX11* mutations in 3 additional patients with SPTCLs (SP32, SP47, and SP51) and 1 patient with PCGDTCL (GD3). All SPTCL cases with *DDX11* mutations had the *HAVCR2*<sup>Y82C</sup> genotype. Notably, patient SP47 was heterozygous for *HAVCR2*<sup>Y82C</sup> and harbored the oncogenic hotspot mutation *IDH1* R132C. No structural variants were detected by using WES, TGS, or RNA-sequencing.

To compare the genetic features of *HAVCR2*<sup>Y82C</sup> with those of *HAVCR2*<sup>WT</sup> SPTCLs, we extended our data set by integrating 2 previously published WES data sets<sup>5,6</sup> (Figure 2). Mutations in *ASXL1*, *CAPN1*, *UNC13D*, *PIAS3*, *PIK3CD*, *KMT2D*, and *BRD2* were significantly more frequent in patients with *HAVCR2*<sup>WT</sup> SPTCL than in those with *HAVCR2* mutations.

**Table 1. Clinicopathological characteristics of SPTCLs according to *HAVCR2* genotype**

Characteristic	WT	Y82C	Unknown	Total	P
<b>Clinical features</b>					
Age					
Median (range), y	40 (16-74)	26 (8-62)	52 (35-68)	32 (8-74)	.002*
<30 y	6 (25.0%)	18 (72.0%)	0 (0.0%)	24 (45.3%)	.001†
≥30 y	18 (75.0%)	7 (28.0%)	4 (100.0%)	29 (54.7%)	
Sex					
Male	6 (25.0%)	9 (36.0%)	1 (25.0%)	16 (30.2%)	.404‡
Female	18 (75.0%)	16 (64.0%)	3 (75.0%)	37 (69.8%)	
HLH/HLH-like systemic illness					
No	22 (95.7%)	11 (45.8%)	2 (100.0%)	35 (71.4%)	<.001†
Yes	1 (4.3%)	13 (54.2%)	0 (0.0%)	14 (28.6%)	
BM involvement					
Absent	21 (100.0%)	12 (95.7%)	0 (0.0%)	43 (93.5%)	1.000‡
Present	0 (0.0%)	1 (4.3%)	2 (100.0%)	3 (6.5%)	
First-line treatments					
Chemotherapy	16 (88.9%)	14 (63.6%)	3 (100.0%)	33 (76.7%)	.069‡
Immunosuppressive	2 (11.1%)	8 (36.4%)	0 (0.0%)	10 (23.3%)	
HSCT§					
No	8 (80.0%)	3 (33.3%)	2 (100.0%)	13 (61.9%)	.070‡
Yes	2 (20.0%)	6 (66.7%)	0 (0.0%)	8 (38.1%)	
Relapse					
No	17 (73.9%)	14 (60.9%)	3 (100.0%)	34 (69.4%)	.345†
Yes	6 (26.1%)	9 (39.1%)	0 (0.0%)	15 (30.6%)	
5-y RFS					
Median (range), m	57 (1-60)	11 (1-60)	60 (16-60)	30 (1-60)	.001*
Death					
No	21 (87.5%)	21 (87.5%)	3 (100.0%)	45 (88.2%)	1.000‡
Yes	3 (12.5%)	3 (12.5%)	0 (0.0%)	6 (11.8%)	
5-y OS					
Median (range), m	60 (2-60)	25 (1-60)	60 (16-60)	39 (1-60)	.004*
5-y DSS					
Median (range), m	59.5 (2-60)	19 (1-60)	60 (16-60)	37 (1-60)	.003*
<b>Histopathological features</b>					
Necrosis					
Absent	14 (66.7%)	13 (52.0%)	1 (50.0%)	28 (58.3%)	.314†
Present	7 (33.3%)	12 (48.0%)	1 (50.0%)	20 (41.7%)	
Granulomatous inflammation					
Absent	17 (81.0%)	25 (100.0%)	2 (100.0%)	44 (91.7%)	.037‡
Present	4 (19.0%)	0 (0.0%)	0 (0.0%)	4 (8.3%)	
Lipogranuloma					
Absent	16 (76.2%)	22 (88.0%)	2 (100.0%)	40 (83.3%)	.293‡
Present	5 (23.8%)	3 (12.0%)	0 (0.0%)	8 (16.7%)	
pSTAT3 IHC					
Low	12 (70.6%)	4 (25.0%)	0 (0.0%)	16 (48.5%)	.015†
High	5 (29.4%)	12 (75.0%)	0 (0.0%)	17 (51.5%)	

BM, bone marrow; DSS, disease-specific survival; HLH, hemophagocytic lymphohistiocytosis; HSCT, hematopoietic stem cell transplantation; OS, overall survival; RFS, relapse-free survival.  
 \*Compared between *HAVCR2*<sup>WT</sup> and *HAVCR2*<sup>Y82C</sup> by using the Mann-Whitney *U* test.

†Compared between *HAVCR2*<sup>WT</sup> and *HAVCR2*<sup>Y82C</sup> by using the  $\chi^2$  test.

‡Compared between *HAVCR2*<sup>WT</sup> and *HAVCR2*<sup>Y82C</sup> by using Fisher's exact test.

§Either autologous or allogeneic transplantation.

||Used median values as cutoffs.



**Table 1. (continued)**

Characteristic	WT	Y82C	Unknown	Total	P
CCR4 IHC <sup>‡</sup>					.019†
Low	5 (27.8%)	12 (66.7%)	0 (0.0%)	17 (47.2%)	
High	13 (72.2%)	6 (33.3%)	0 (0.0%)	19 (52.8%)	
<b>Total</b>	<b>24 (45.3%)</b>	<b>25 (47.2%)</b>	<b>4 (7.5%)</b>	<b>53 (100.0%)</b>	

BM, bone marrow; DSS, disease-specific survival; HLH, hemophagocytic lymphohistiocytosis; HSCT, hematopoietic stem cell transplantation; OS, overall survival; RFS, relapse-free survival.

\*Compared between *HAVCR2*<sup>WT</sup> and *HAVCR2*<sup>Y82C</sup> by using the Mann-Whitney *U* test.

†Compared between *HAVCR2*<sup>WT</sup> and *HAVCR2*<sup>Y82C</sup> by using the  $\chi^2$  test.

‡Compared between *HAVCR2*<sup>WT</sup> and *HAVCR2*<sup>Y82C</sup> by using Fisher's exact test.

§Either autologous or allogeneic transplantation.

||Used median values as cutoffs.

### Enrichment of inflammation-related pathways in *HAVCR2*<sup>Y82C</sup> SPTCLs

We used RNA-sequencing data from the discovery set to conduct GSEA and compare involved pathways between *HAVCR2*<sup>Y82C</sup> and *HAVCR2*<sup>WT</sup> SPTCLs (Figure 3A-B; supplemental Table 10). Significantly enriched pathways in *HAVCR2*<sup>Y82C</sup> SPTCL included tumor necrosis factor- $\alpha$  signaling via NF- $\kappa$ B (normalized enrichment score [NES] = 1.841; FDR q-value = 0.008), hypoxia (NES = 1.860; FDR q-value = 0.009), IL6-JAK-STAT3 signaling (NES = 1.679; FDR q-value = 0.026), apoptosis (NES = 1.437; FDR q-value = 0.121), and MTORC1 signaling (NES = 1.322; FDR q-value = 0.188).

We performed pSTAT3 IHC, and the number of pSTAT3-positive cells was significantly higher in *HAVCR2*<sup>Y82C</sup> SPTCLs compared with *HAVCR2*<sup>WT</sup> ( $P = .031$ ) (Figure 3C; supplemental Table 11); pSTAT3 positivity was observed in reactive cells within the tumor microenvironment as well as adipocyte rimming tumor cells.

Moreover, gene sets associated with T-cell activation mediated by calcium signaling and NFAT nuclear translocation<sup>18</sup> were enriched in *HAVCR2*<sup>Y82C</sup> SPTCLs (TCELL\_PIIND\_CSADOWN4X and TCELL\_PIIND\_CALCIUMDEFPTDOWN4X\_FESKE\_FIG6; NES = 1.727 and 1.728; FDR q-values = 0.034 and 0.042, respectively). Genes associated with NF- $\kappa$ B subunits on lymphocytic stimulation (NFKB\_CHIPCHIP\_YOUNG\_4FACTORS)<sup>19</sup> were significantly enriched in *HAVCR2*<sup>Y82C</sup> (NES = 1.408; FDR q-value = 0.235). Taken together, the GSEA results imply that compared with *HAVCR2*<sup>WT</sup> SPTCLs, *HAVCR2*<sup>Y82C</sup> SPTCLs exhibit enhanced inflammatory responses.

### *HAVCR2*<sup>WT</sup> SPTCLs are characterized by upregulation of genes involved in lymphocyte homing and immune regulation

To obtain further insight into the role of *HAVCR2* mutations in SPTCL pathobiology, we identified DEGs between SPTCL subtypes. A total of 52 DEGs were identified between *HAVCR2*<sup>Y82C</sup> and *HAVCR2*<sup>WT</sup> SPTCLs (Figure 3D); *IL1R2* and 20 other genes were upregulated in *HAVCR2*<sup>Y82C</sup> SPTCLs. Genes associated with lymphocyte homing (*CCR4* and *GPR183*) and autoimmunity (*STAB2*) were among the 31 genes that were significantly upregulated in *HAVCR2*<sup>WT</sup> SPTCLs.

CCR4 expression in regulatory T cells (Tregs) residing in nonlymphoid organs has previously been reported<sup>20</sup>; thus, we evaluated differences in CCR4 and Foxp3 expression between *HAVCR2*<sup>Y82C</sup> and *HAVCR2*<sup>WT</sup> SPTCLs (Figure 3E-G). The number of CCR4-positive

cells was significantly higher in *HAVCR2*<sup>WT</sup> SPTCLs than in *HAVCR2*<sup>Y82C</sup> SPTCLs ( $P = .029$ ) (Figure 3F; supplemental Table 11). Microscopic examination revealed that most of the CCR4-positive cells appeared to be distinct from adipocyte-rimming CD8-positive cells (Figure 3F, inset), implying that these CCR4-positive cells were reactive cells within the microenvironment rather than neoplastic cells.

The percentages of Foxp3-positive cells and CCR4-positive cells showed a trend toward positive correlation (Spearman's  $\rho = 0.318$  and  $P = .081$  when excluding outlier results) (Figure 3E), and Foxp3-positive Tregs were more abundant in *HAVCR2*<sup>WT</sup> SPTCLs ( $P = .033$ ) (Figure 3G). However, the percentages of Foxp3-positive cells were significantly lower than those of CCR4-positive cells (paired Student *t* test,  $P = .001$ ). Double-staining for Foxp3 and CCR4 on selected samples revealed that not all CCR4-positive cells coexpressed Foxp3 (Figure 4). This observation suggests that non-Treg CCR4-positive cells reside in the tumor microenvironment, especially among *HAVCR2*<sup>WT</sup> SPTCLs.

### Clinicopathological risk score for the prognostic stratification of SPTCLs

Patient characteristics and clinical follow-up data are summarized in supplemental Figure 4. RFS analyses according to various clinicopathological variables (Figure 5A-F; supplemental Figure 5) revealed that *HAVCR2*<sup>Y82C</sup> mutations and age <30 years were significantly associated with a poor prognosis ( $P = .023$  and  $P = .033$ , respectively). In contrast, necrosis, pSTAT3-positivity, CCR4-positivity, HLH/HLH-like systemic illness, and bone marrow involvement had no significant prognostic value. No clinicopathological factors were significantly associated with OS (supplemental Figure 6).

We used age <30 years (score 1) and *HAVCR2*<sup>Y82C</sup> (score 1) to build a risk scoring system for the prognostic stratification of patients with SPTCLs. The distribution of the 49 patients was as follows: score 0, 18 patients (36.7%; median RFS, 47 months; range, 1-190 months); score 1, 13 patients (26.5%; median RFS, 37 months; range, 6-119 months); and score 2, 18 patients (36.7%; median RFS, 10 months; range, 1-53 months). This risk score was significantly associated with patient outcomes ( $P = .031$ ) (Figure 5G), and patients with higher score experienced HLH/HLH-like systemic illness more frequently ( $P = .005$ ) (Figure 5H). We assessed the association between the risk score and events of HLH/HLH-like illness using the previously published clinical data,<sup>5,6</sup> which revealed similarly significant results ( $P < .001$ ).

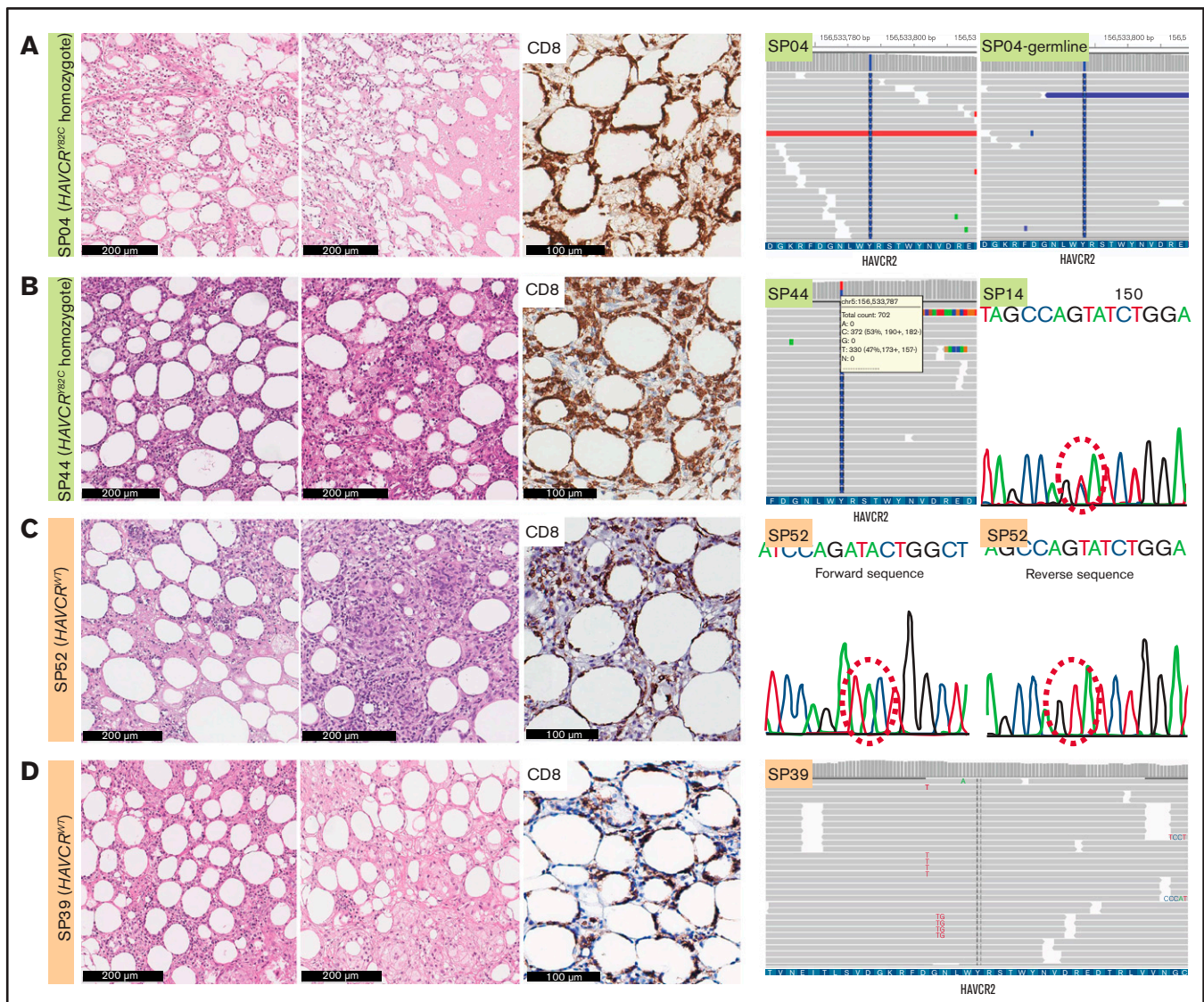


**Figure 1. Histopathological features of SPTCLs and detection of *HAVCR2*<sup>Y82C</sup> mutations.** (A) Excisional biopsy specimen of a 16-year-old female patient with an SPTCL (SP04) exhibited adipocytic rimming by CD8-positive lymphocytes along with prominent necrosis. This patient was confirmed by using WES to have a germline homozygous *HAVCR2*<sup>Y82C</sup> mutation. (B) Lipogranulomatous inflammation was observed in a 54-year-old female patient (SP44), and TGS revealed heterozygous *HAVCR2*<sup>Y82C</sup> mutations. SP14 harbored heterozygous *HAVCR2*<sup>Y82C</sup> mutations, which could be inferred from double peaks on the electropherogram. (C) A 45-year-old female patient (SP52) with the *HAVCR2*<sup>WT</sup> genotype had both necrosis and granuloma formation. (D) Lipogranulomatous inflammation was observed in the *HAVCR2*<sup>WT</sup> SPTCL of a 53-year-old woman (SP39).

## Discussion

We established a nationwide cohort of patients with SPTCLs and assessed the characteristics of patients with *HAVCR2* mutations. We identified differentially enriched cellular pathways and microenvironmental factors according to *HAVCR2* genotype by high-throughput sequencing and developed a prognostication score.

To our knowledge, this study is the first to confirm germline *HAVCR2*<sup>Y82C</sup> mutations in Korean patients with SPTCLs and is the largest cohort study of East Asian patients with SPTCLs. We provide strong evidence that patients with *HAVCR2*<sup>Y82C</sup> SPTCLs exhibit unique clinical features, including younger age, frequent HLH/HLH-like systemic illness, and shorter RFS; some of these findings were previously reported<sup>5,7</sup> or failed to be confirmed.<sup>6,7</sup> By performing

TGS in patients with MF, PCGDTCL, and LP, we showed that the *HAVCR2*<sup>Y82C</sup> mutation might be a unique feature of SPTCL.

Four (8.2%) of 49 patients were identified with heterozygous *HAVCR2*<sup>Y82C</sup> mutations. One patient with heterozygous *HAVCR2*<sup>I97M</sup> was previously reported by Gayden et al,<sup>5</sup> and compound heterozygotes with *HAVCR2*<sup>Y82C/I97M</sup> and *HAVCR2*<sup>Y82C/T101I</sup> have been described.<sup>5,6</sup> However, heterozygous *HAVCR2*<sup>Y82C</sup> mutations have not been previously reported. A careful review of the histopathological features and IHC results revealed that there were no significant differences between these four patients and patients with homozygous *HAVCR2*<sup>Y82C</sup> mutations. Regarding clinical features, heterozygous *HAVCR2*<sup>Y82C</sup> patients were less likely complicated by HLH/HLH-like systemic illness, which is compatible with the previous

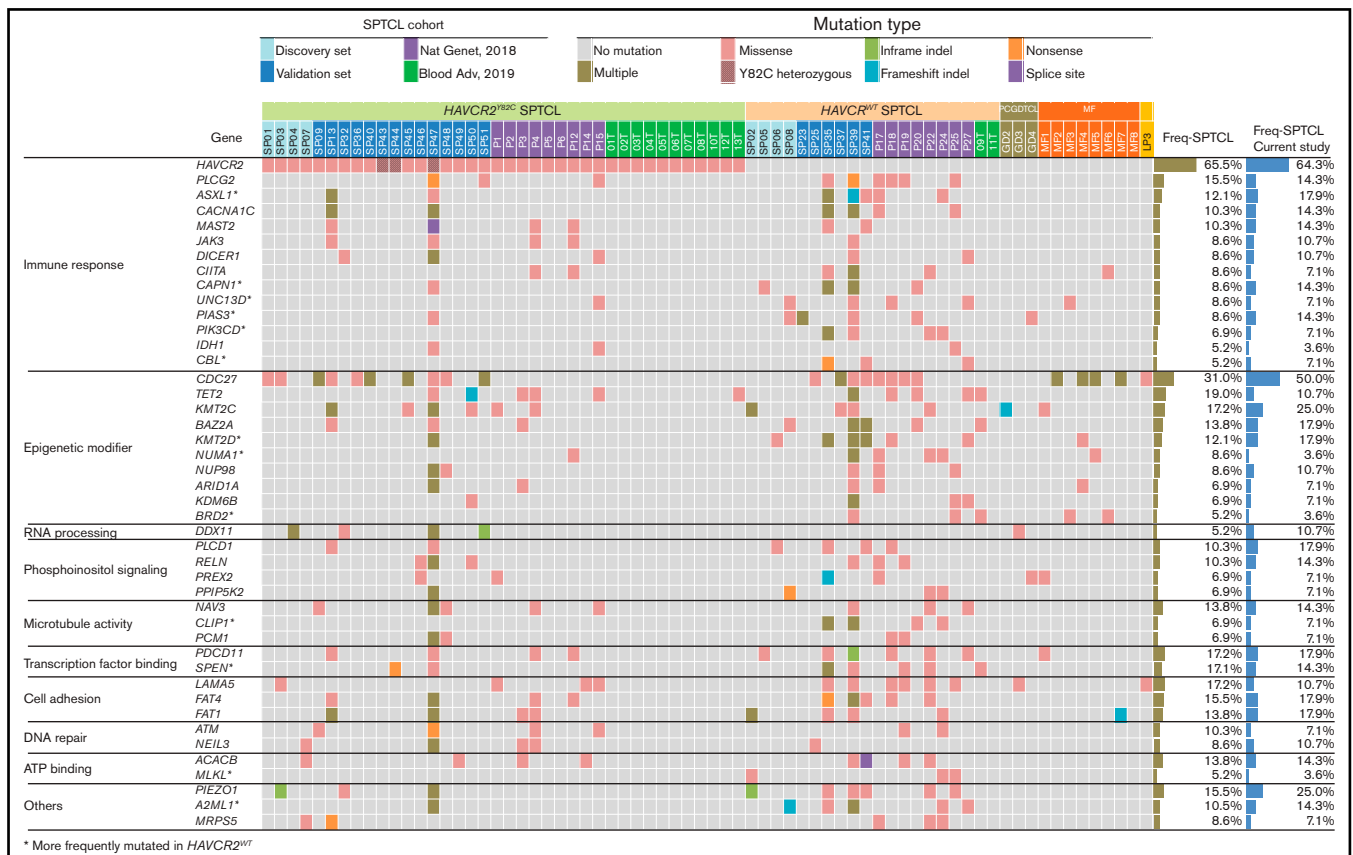


**Figure 2. Mutational landscape of SPTCLs and other cutaneous T-cell lymphomas with panniculitic presentation in Korean patients.** Integrated mutation map of Korean SPTCLs and previously reported data sets. A subset of genetic alterations was shared with PCGDTCL and MFs; however, the *HAVCR2*<sup>Y82C</sup> mutation was seen exclusively in SPTCLs. Genes that were more frequently mutated in *HAVCR2*<sup>WT</sup> SPTCLs are indicated with asterisks; statistical significance was determined by using Fisher's exact test. ATP, adenosine triphosphate.

finding that tumor cells of heterozygous *HAVCR2*<sup>Y82C</sup> patients exhibited intermediate membranous TIM-3 expression.<sup>5</sup> However, survival analyses of various clinicopathological factors after excluding these 4 heterozygous *HAVCR2*<sup>Y82C</sup> patients revealed no significant differences in patients' prognosis compared with our original analyses on the whole study population (data not shown). Considering the minor allele frequency of *HAVCR2*<sup>Y82C</sup> in East Asian subjects is reportedly as high as 0.0036,<sup>6</sup> we consider that monoallelic *HAVCR2*<sup>Y82C</sup> alterations alone are not sufficient to cause SPTCL. We sought to identify additional factors contributing to disease presentation; however, no recurrent genetic alterations were found in this subset. Further studies on a larger cohort of patients harboring heterozygous *HAVCR2*<sup>Y82C</sup> mutations are required to elucidate the possible genetic or epigenetic events that contribute to SPTCL development and the clinicopathological implication of heterozygous *HAVCR2*<sup>Y82C</sup> mutations.

Little is known about the somatic mutational profiles of SPTCLs, especially those with the *HAVCR2*<sup>WT</sup> genotype. By combining our data with published data set, we found that certain genetic alterations were significantly more frequent in *HAVCR2*<sup>WT</sup> than in *HAVCR2*<sup>MUT</sup> SPTCLs. For instance, 14.3% (4 of 28) of the study population harbored mutations in *PIAS3*, the gene-encoding protein inhibitor of activated STAT3 (*PIAS3*), the main inhibitor of *STAT3*<sup>21</sup>; among these

patients, 3 were *HAVCR2*<sup>WT</sup>. In addition to the *STAT* pathway, *NF-κB* signaling is also affected by *PIAS3*.<sup>22,23</sup> Although the functional effects of the *PIAS3* mutations identified in this study remain to be determined, aberrant *PIAS3* function may deregulate immune pathways and contribute to the pathogenesis of SPTCLs in the absence of deleterious *HAVCR2* mutations.

*UNC13D* missense mutations were more frequent in *HAVCR2*<sup>WT</sup> SPTCLs. Even though *UNC13D* mutations have been implicated in atypical familial HLH in some Korean patients,<sup>24,25</sup> two women in our cohort (SP08 and SP39) were not complicated by HLH. A recent study of Swedish patients suggested that the haploinsufficiency of *UNC13D* caused by inversion was associated with an increased risk of lymphoma, especially in women.<sup>26</sup> The mechanisms linking *UNC13D* mutations to the pathogenesis of *HAVCR2*<sup>WT</sup> SPTCL remain to be unveiled.

Patient SP04 harbored 2 somatic mutations in the DEAD-domain of *DDX11*, which encodes an RNA helicase family member involved in a rare congenital disease called Warsaw breakage syndrome.<sup>27</sup> We identified *DDX11* mutations in four *HAVCR2*<sup>Y82C</sup> SPTCLs (4 of 25 [16.0%]) and one PCGDTCL (1 of 3 [33.3%]). Mutations in RNA helicase family members have been extensively studied in extranodal NK/T-cell lymphomas<sup>28</sup>; nevertheless, *DDX11* alterations have not been described in extranodal NK/T-cell lymphomas or SPTCLs. Of



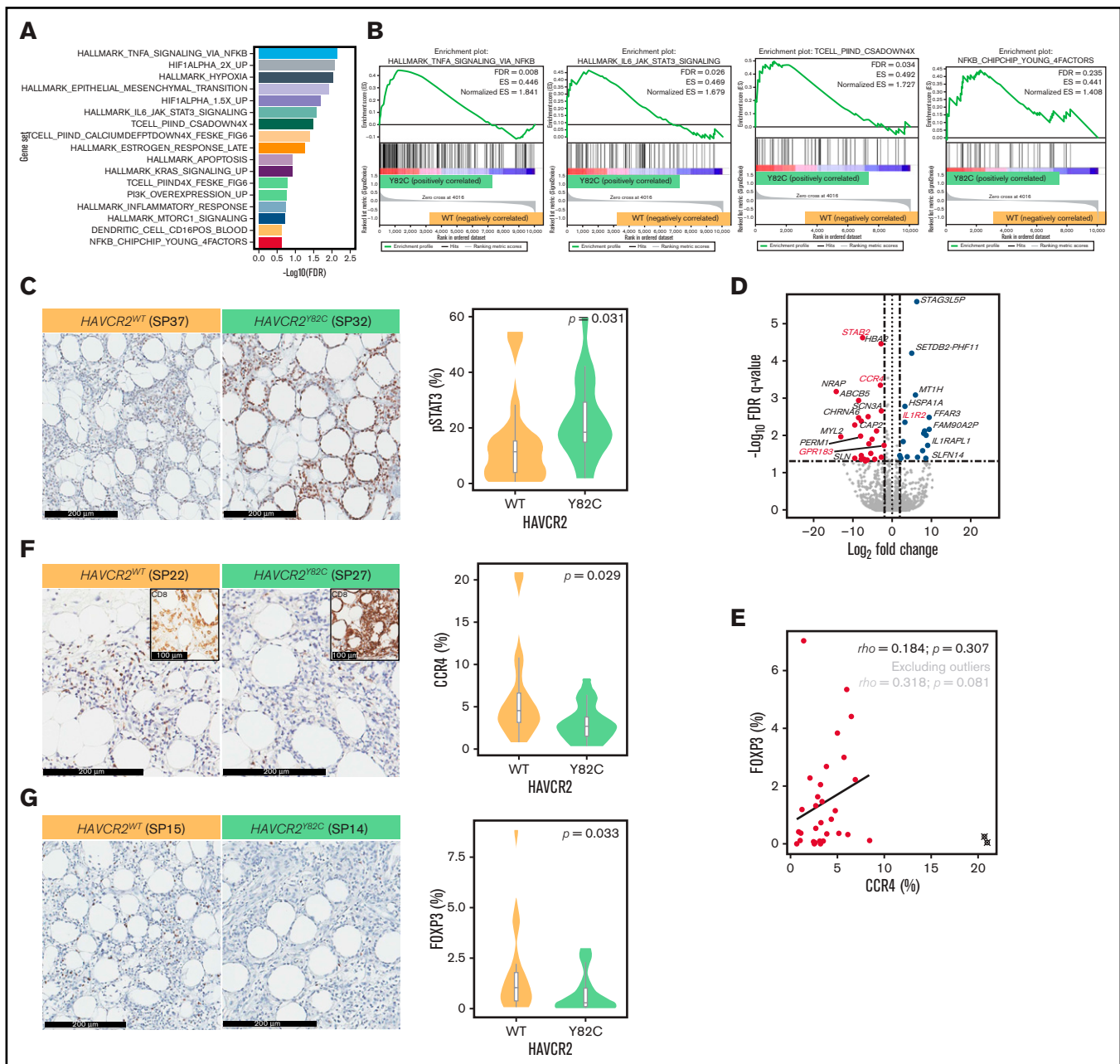


**Figure 3. GSEA and DEGs between *HAVCR2*<sup>Y82C</sup> and *HAVCR2*<sup>WT</sup> SPTCLs.** (A) Significantly enriched gene sets in *HAVCR2*<sup>Y82C</sup> SPTCLs and their NES are shown. (B) Most enriched gene set in *HAVCR2*<sup>Y82C</sup> SPTCLs were associated with increased inflammatory responses. (C) Higher number of pSTAT3-positive cells characterizes *HAVCR2*<sup>Y82C</sup> SPTCLs. (D) Volcano plot highlighting 52 genes differentially expressed according to *HAVCR2* genotype. (E) CCR4 and Foxp3 positivity was assessed by using IHC. Correlation plot showing percentages of CCR4- and Foxp3-positive cells; circled cross indicates outlier results. (F and G) *HAVCR2*<sup>WT</sup> SPTCLs had a significantly higher number of CCR4-positive cells and Foxp3-positive cells compared with *HAVCR2*<sup>Y82C</sup> SPTCLs (Mann-Whitney *U* test).

note, *DDX11* rearrangements have been associated with diffuse large B-cell lymphoma-associated HLH.<sup>29</sup> Furthermore, B-cell lymphoma cell lines strongly depended on *DDX11*,<sup>30</sup> although its role in T-cell lymphomagenesis remains largely unknown.

Comparative analyses between *HAVCR2*<sup>Y82C</sup> and *HAVCR2*<sup>WT</sup> SPTCLs using RNA-sequencing revealed profound differences between the 2 SPTCL subsets. *HAVCR2*<sup>Y82C</sup> SPTCLs were enriched in inflammation-associated cellular pathways, including

IL6-JAK-STAT3, further supported by the higher number of pSTAT3-positive cells among *HAVCR2*<sup>Y82C</sup> SPTCLs on IHC; pSTAT3 was positive in adipocytic rimming tumor cells and reactive cells, which suggests that activation of the IL6-JAK-STAT pathway could be attributable to both tumor and microenvironmental factors. Upregulation of NF-κB signaling and hypoxia-related genes was also observed, implying uncontrolled immune activation within the tumor milieu. Of note, enrichment of gene sets regulated by calcium



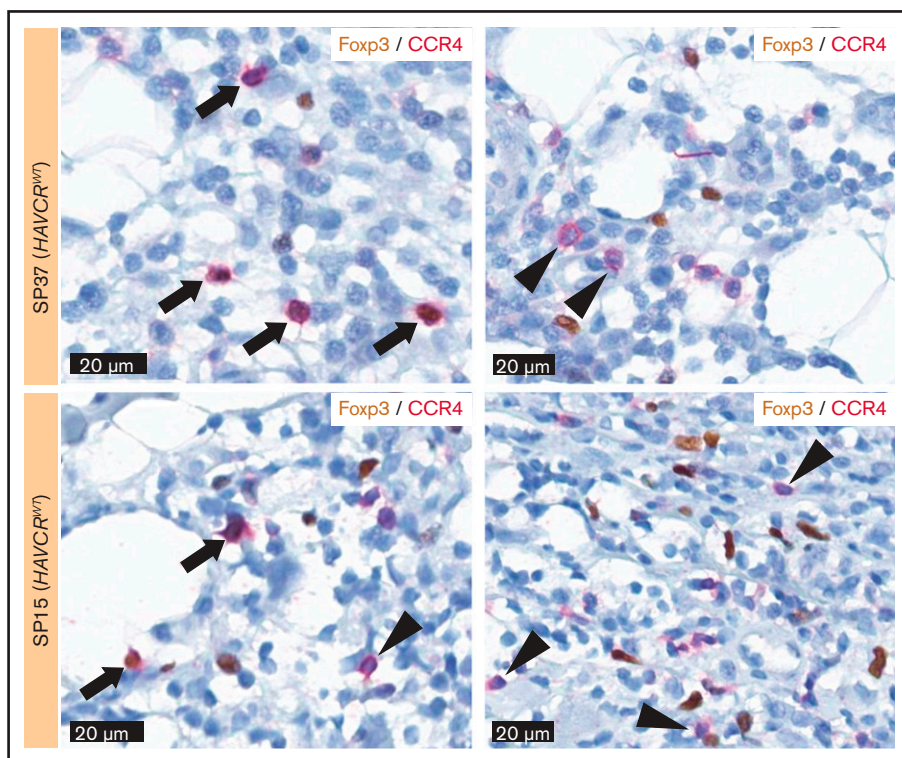


**Figure 4. Double-staining for Foxp3 and CCR4.** Double-staining showed the cells coexpressing Foxp3 and CCR4 (arrow) as well as the cells only positive for CCR4 (arrowhead), suggesting the presence of non-Treg CCR4-positive cells within the tumor microenvironment of SPTCL.

signaling in T-lymphocytes underpins the crucial role of activated T cells in SPTCL pathogenesis.

We observed a marked increase in *CCR4* expression levels in *HAVCR2*<sup>WT</sup> SPTCLs, and numbers of CCR4-positive cells and Foxp3-positive cells were significantly higher in the tumor microenvironment of *HAVCR2*<sup>WT</sup> SPTCLs, consistent with a previous study showing decreased Foxp3<sup>+</sup> Tregs in *HAVCR2*<sup>MUT</sup> SPTCLs.<sup>5</sup> CCR4 is a chemokine receptor that regulates Treg homing in nonlymphoid tissues, including the skin<sup>31,32</sup>; loss of CCR4 expression on the Treg compartment resulted in severe inflammatory disease in mouse skin.<sup>20</sup> Therefore, in the tumor microenvironment of *HAVCR2*<sup>WT</sup> SPTCLs, cytotoxic T cells may be partly controlled by intact CCR4-mediated Treg activity, whereas lack of local immune regulation in *HAVCR2*<sup>Y82C</sup> SPTCLs may result in systemic propagation of severe inflammation.

Numbers of CCR4-positive cells were greater than Foxp3-positive cells, and not all CCR4-positive cells coexpressed Foxp3 according to the double-staining; these findings suggested the presence of a non-Treg CCR4-positive cell population. Considering that CCR4 is also a chemoattractant receptor on the T helper 2 cells,<sup>33</sup> we performed double-staining for GATA3 and CCR4, in which we observed that some cells were positive for both, whereas others were not (data not shown). Taken together, these findings suggested that a subset of non-Treg CCR4-positive cells could be attributed to the T helper 2 category.

Previous studies have shown HLH to be the most important factor indicating a poor prognosis in SPTCL, yet robust prognostic factors in SPTCL are lacking.<sup>3,34</sup> Although HLH alone tended to correlate with poor RFS in the study population, it did not reach statistical

significance. Notably, *HAVCR2*<sup>Y82C</sup> mutations and younger age were significantly associated with a poor prognosis. We established a risk score system by integrating these 2 factors, which robustly predicted shorter RFS and more frequent events of systemic complication. Although this system showed no significant prognostic impact on patients' OS, significant association of RFS, events of systemic complication according to our risk score, imply that this system could aid in clinical management and proper triage of the patients with SPTCL. However, because the 2 factors accounting for this score system are closely associated, additional validation in an independent cohort is required to confirm the prognostic value and validity.

Most of the mutational analyses in this study were based on tumor-only sequencing; therefore, copy number analyses were not feasible, and we could not precisely confirm the germline *HAVCR2* genotype in most patients. However, we could infer the germline nature of *HAVCR2* mutation based on the patterns of VAFs, which approximated to either 50.0% or 100.0%, whereas VAFs of other mutations varied widely. On targeted sequencing, some samples showed an exceptionally high number of variants, implying the possibility of false-positive findings. However, we implemented a thorough variant-filtering process to reduce false-positive findings, as detailed in the supplemental Methods. In addition, not all samples in this cohort were suitable for high-quality next-generation sequencing, and therefore limited genetic information was available from those who underwent direct sequencing of *HAVCR2* exon 2 only. Nevertheless, by integrating a previously published data set, we sought to provide a novel insight into the genetics of SPTCLs. Although RNA-sequencing was performed on only a limited number of samples, we performed comparative analyses of SPTCLs according to *HAVCR2* genotype

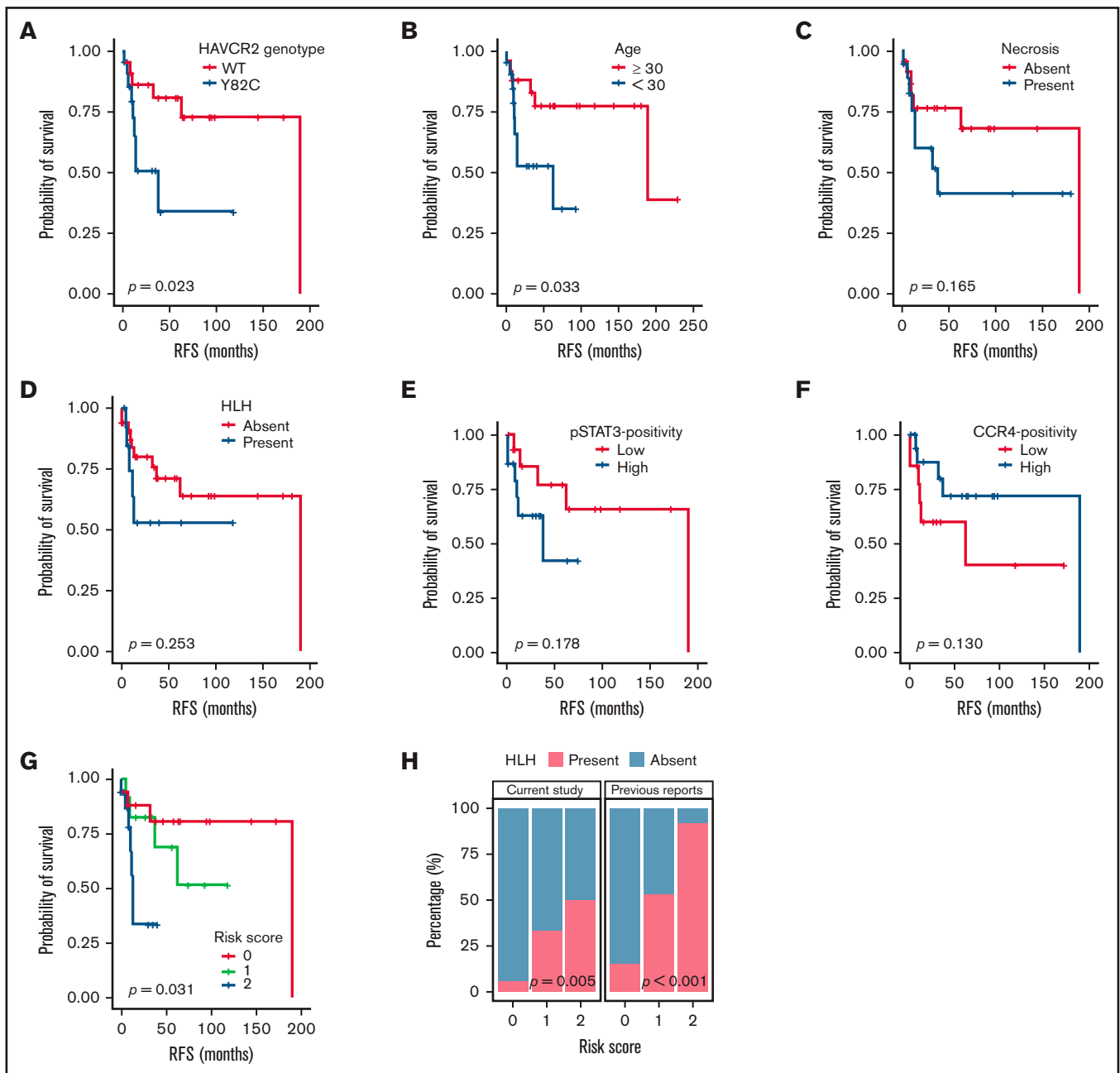


**Figure 5. Survival analyses according to clinicopathological factors and development of an SPTCL risk stratification score.** (A and B) The presence of the *HAVCR2*<sup>Y82C</sup> mutation and age  $< 30$  years at diagnosis, respectively, were significant prognostic factors in patients with SPTCLs. (C) A tendency toward poor outcomes was observed in patients with tissue necrosis. (D-F) HLH (or HLH-like systemic illness), pSTAT3 positivity, and lower CCR4 expression were not significantly associated with RFS. (G) The risk score system integrating patients' age and *HAVCR2* status was significantly associated with RFS ( $P = .031$ ). Patients with score 2 had a shorter RFS compared with patients with score 0 (log-rank test,  $P = .024$ ). However, there were no significant differences between scores 2 vs 1 and scores 1 vs 2 (log-rank test,  $P = .068$  and  $0.354$ , respectively). (H) Significant correlation between the risk score and event of systemic complication was observed in the current study population ( $P = .005$ , linear-by-linear test) as well as in the pooled analysis using the published data from Gayden et al<sup>5</sup> and Polprasert et al<sup>6</sup> ( $P < .001$ , linear-by-linear test).

and validated the findings by IHC in extended samples, thereby gaining more insight into the biology of this rare disease.

In conclusion, using various sequencing strategies, we assessed the epidemiology and clinicopathological implications of *HAVCR2* mutations in a nationwide cohort of Korean patients with SPTCL. Differential distribution of somatic mutations and gene expression

profiles according to *HAVCR2* genotype were identified. Notably, inflammatory signaling pathways via tumor necrosis factor- $\alpha$  and IL6-JAK-STAT3 axis were enriched in *HAVCR2*<sup>Y82C</sup> SPTCLs, whereas a CCR4-rich milieu was observed in *HAVCR2*<sup>WT</sup> SPTCLs, enhancing our current understanding of SPTCL pathogenesis. Additional validation of our proposed risk score may provide a

valuable and easy-to-implement tool for the prognostic stratification of patients with SPTCLs.

## Acknowledgments

This work was supported by the Basic Science Research through the National Research Foundation of Korea (NRF) funded by the Ministry of Education, Science and Technology Program (grant NRF-2016R1D1A1B01015964), and the Basic Research Program through the NRF funded by the Ministry of Science and ICT (grant 2020R1A4A1017515) and the Seoul National University Hospital Research (grant 0420190470).

## Authorship

Contribution: Y.K.J. designed and supervised the project; J.K., I.J., and K.K. performed bioinformatics analyses; J.K. and S.M.

performed the experiments; J.K. and Y.K.J. analyzed the results; C.L., H.J.C., Y.H.O., J.-M.K., J.H.H., J.H.P., J.C., Y.H.K., C.-S.P., H.G., J.H., and Y.K.J. contributed to the sample preparation and review of clinical data and pathology; and J.K. and Y.K.J. wrote the manuscript; and all authors read and approved the final manuscript.

Conflict-of-interest disclosure: The authors declare no competing financial interests.

ORCID profiles: I.J., 0000-0001-9542-6984; C.L., 0000-0001-5098-8529; Y.H.O., 0000-0001-8750-9843; H.G., 0000-0003-0412-8709; Y.K.J., 0000-0001-8466-9681.

Correspondence: Yoon Kyung Jeon, Department of Pathology, Seoul National University Hospital, Seoul National University College of Medicine, 101 Daehak-ro, Jongno-gu, Seoul 03080, Republic of Korea; e-mail: ykjeon@snu.ac.kr.

## References

1. Swerdlow SH, Campo E, Pileri SA, et al. The 2016 revision of the World Health Organization classification of lymphoid neoplasms. *Blood*. 2016; 127(20):2375-2390.
2. Jung HR, Huh J, Ko Y-H, et al. Classification of malignant lymphoma subtypes in Korean patients: a report of the 4th nationwide study. *J Hematop*. 2019; 12(4):173-181.
3. Willemze R, Jansen PM, Cerroni L, et al; EORTC Cutaneous Lymphoma Group. Subcutaneous panniculitis-like T-cell lymphoma: definition, classification, and prognostic factors: an EORTC Cutaneous Lymphoma Group Study of 83 cases. *Blood*. 2008;111(2):838-845.
4. Willemze R. Cutaneous lymphomas with a panniculitic presentation. *Semin Diagn Pathol*. 2017;34(1):36-43.
5. Gayden T, Sepulveda FE, Khuong-Quang D-A, et al. Germline HAVCR2 mutations altering TIM-3 characterize subcutaneous panniculitis-like T cell lymphomas with hemophagocytic lymphohistiocytic syndrome [published correction appears in *Nat Genet*. 2019;51(1):196]. *Nat Genet*. 2018; 50(12):1650-1657.
6. Polprasert C, Takeuchi Y, Kakiuchi N, et al. Frequent germline mutations of HAVCR2 in sporadic subcutaneous panniculitis-like T-cell lymphoma. *Blood Adv*. 2019;3(4):588-595.
7. Sonigo G, Battistella M, Beylot-Barry M, et al. HAVCR2 mutations are associated with severe hemophagocytic syndrome in subcutaneous panniculitis-like T-cell lymphoma. *Blood*. 2020;135(13):1058-1061.
8. Monney L, Sabatos CA, Gaglia JL, et al. Th1-specific cell surface protein Tim-3 regulates macrophage activation and severity of an autoimmune disease. *Nature*. 2002;415(6871):536-541.
9. Henter JI, Horne A, Aricó M, et al. HLH-2004: diagnostic and therapeutic guidelines for hemophagocytic lymphohistiocytosis. *Pediatr Blood Cancer*. 2007;48(2):124-131.
10. Li Z, Lu L, Zhou Z, et al. Recurrent mutations in epigenetic modifiers and the PI3K/AKT/mTOR pathway in subcutaneous panniculitis-like T-cell lymphoma. *Br J Haematol*. 2018;181(3):406-410.
11. Fernandez-Pol S, Costa HA, Steiner DF, et al. High-throughput sequencing of subcutaneous panniculitis-like T-cell lymphoma reveals candidate pathogenic mutations. *Appl Immunohistochem Mol Morphol*. 2019;27(10):740-748.
12. da Silva Almeida AC, Abate F, Khiabani H, et al. The mutational landscape of cutaneous T cell lymphoma and Sézary syndrome. *Nat Genet*. 2015; 47(12):1465-1470.
13. Subramanian A, Tamayo P, Mootha VK, et al. Gene set enrichment analysis: a knowledge-based approach for interpreting genome-wide expression profiles. *Proc Natl Acad Sci USA*. 2005;102(43):15545-15550.
14. Yoon S, Kim S-Y, Nam D. Improving Gene-Set Enrichment Analysis of RNA-seq data with small replicates. *PLoS One*. 2016;11(11):e0165919.
15. Liberzon A, Birger C, Thorvaldsdóttir H, Ghandi M, Mesirov JP, Tamayo P. The Molecular Signatures Database (MSigDB) hallmark gene set collection. *Cell Syst*. 2015;1(6):417-425.
16. Shaffer AL, Wright G, Yang L, et al. A library of gene expression signatures to illuminate normal and pathological lymphoid biology. *Immunol Rev*. 2006; 210(1):67-85.
17. Love MI, Huber W, Anders S. Moderated estimation of fold change and dispersion for RNA-seq data with DESeq2. *Genome Biol*. 2014;15(12):550.
18. Feske S, Giltner J, Dolmetsch R, Staudt LM, Rao A. Gene regulation mediated by calcium signals in T lymphocytes [published correction appears in *Nat Immunol*. 2008;9(3):328-329]. *Nat Immunol*. 2001;2(4):316-324.



19. Schreiber J, Jenner RG, Murray HL, Gerber GK, Gifford DK, Young RA. Coordinated binding of NF-kappaB family members in the response of human cells to lipopolysaccharide. *Proc Natl Acad Sci USA*. 2006;103(15):5899-5904.
20. Sather BD, Treuting P, Perdue N, et al. Altering the distribution of Foxp3(+) regulatory T cells results in tissue-specific inflammatory disease. *J Exp Med*. 2007;204(6):1335-1347.
21. Chung CD, Liao J, Liu B, et al. Specific inhibition of Stat3 signal transduction by PIAS3. *Science*. 1997;278(5344):1803-1805.
22. Jang HD, Yoon K, Shin YJ, Kim J, Lee SY. PIAS3 suppresses NF-kappaB-mediated transcription by interacting with the p65/RelA subunit. *J Biol Chem*. 2004;279(23):24873-24880.
23. Liu B, Yang R, Wong KA, et al. Negative regulation of NF-kappaB signaling by PIAS1. *Mol Cell Biol*. 2005;25(3):1113-1123.
24. Yoon HS, Kim HJ, Yoo KH, et al. UNC13D is the predominant causative gene with recurrent splicing mutations in Korean patients with familial hemophagocytic lymphohistiocytosis. *Haematologica*. 2010;95(4):622-626.
25. Rohr J, Beutel K, Maul-Pavicic A, et al. Atypical familial hemophagocytic lymphohistiocytosis due to mutations in UNC13D and STXBP2 overlaps with primary immunodeficiency diseases. *Haematologica*. 2010;95(12):2080-2087.
26. Löfstedt A, Ahlm C, Tesi B, et al. Haploinsufficiency of UNC13D increases the risk of lymphoma. *Cancer*. 2019;125(11):1848-1854.
27. van der Lelij P, Chrzanowska KH, Godthelp BC, et al. Warsaw breakage syndrome, a cohesinopathy associated with mutations in the XPD helicase family member DDX11/ChIR1. *Am J Hum Genet*. 2010;86(2):262-266.
28. Xiong J, Cui B-W, Wang N, et al. Genomic and transcriptomic characterization of natural killer T cell lymphoma. *Cancer Cell*. 2020;37(3):403-419.e6.
29. Patel K, Lee SS, Valasareddy P, Vontela NR, Prouet P, Martin MG. Genetic analysis of B-cell lymphomas associated with hemophagocytic lymphohistiocytosis. *Blood Adv*. 2016;1(3):205-207.
30. Meacham CE, Ho EE, Dubrovsky E, Gertler FB, Hemann MT. In vivo RNAi screening identifies regulators of actin dynamics as key determinants of lymphoma progression. *Nat Genet*. 2009;41(10):1133-1137.
31. Campbell JJ, Haraldsen G, Pan J, et al. The chemokine receptor CCR4 in vascular recognition by cutaneous but not intestinal memory T cells. *Nature*. 1999;400(6746):776-780.
32. Lee I, Wang L, Wells AD, Dorf ME, Ozkaynak E, Hancock WW. Recruitment of Foxp3+ T regulatory cells mediating allograft tolerance depends on the CCR4 chemokine receptor. *J Exp Med*. 2005;201(7):1037-1044.
33. Mikhak Z, Fukui M, Farsidjani A, Medoff BD, Tager AM, Luster AD. Contribution of CCR4 and CCR8 to antigen-specific T(H)2 cell trafficking in allergic pulmonary inflammation. *J Allergy Clin Immunol*. 2009;123(1):67-73.e3.
34. Go RS, Wester SM. Immunophenotypic and molecular features, clinical outcomes, treatments, and prognostic factors associated with subcutaneous panniculitis-like T-cell lymphoma: a systematic analysis of 156 patients reported in the literature. *Cancer*. 2004;101(6):1404-1413.